maging–Based Correction for Partial Volume t Improves Detectability of Intractable ptogenic Foci on Iodine 123 Iomazenil Brain T Images: An Extended Study with a Larger le Size

ORIGINAL RESEARCH

H. Kato
K. Matsuda
K. Baba
E. Shimosegawa
K. Isohashi
M. Imaizumi
J. Hatazawa

UND AND PURPOSE: It has been suggested, on the basis of a previous pilot study conducted number of patients, that MR imaging–based PVE correction in I-123 iomazenil brain SPECT improves the detectability of cortical epileptogenic foci. In the present study, we performed an investigation by using a larger sample size to establish the effectiveness of the PVE correction and to conduct a detailed evaluation based on the histologic classification of lesions.

MATERIALS AND METHODS: Seventy-five patients (male/female, 37/38; age, 28 ± 12 years) with intractable epilepsy who had undergone surgical treatment were enrolled in this study. I-123 iomazenil SPECT and MR imaging examinations were performed before the operation in all patients. I-123 iomazenil SPECT images with and without MR imaging–based PVE correction were assessed visually and by semiquantitative analysis based on the AI(%) of the SPECT count in the resected lesions.

RESULTS: The sensitivity, specificity, and accuracy of foci detection by visual assessment were significantly higher after PVE correction compared with the values obtained before the correction. The results of the semiquantitative analysis revealed that the asymmetry of the SPECT counts was significantly increased after the PVE correction in the surgically resected lesions in cases of mesial temporal sclerosis, tumor, and malformations of cortical development.

CONCLUSIONS: The effectiveness of MR imaging–based PVE correction in I-123 iomazenil brain SPECT in improving the detection of cortical epileptogenic foci with abnormal histologic findings was established by our investigation conducted on a large sample size.

ABBREVIATIONS: AI = asymmetry index; CV = coefficient of variation; EEG = electroencephalogram; GABA = γ-aminobutyric acid; I-123 = iodine 123; MCD = malformations of cortical development; MTS = mesial temporal sclerosis; PVE = partial volume effect

I-123 iomazenil brain SPECT is a functional imaging to detect epileptic foci in patients with intractable epilepsy for whom surgical intervention is considered.[1] I-123 iomazenil is specifically bound to central benzodiazepine receptors,[2] whose attenuation or affinity is known to be reduced in epileptogenic foci.[1,3] In SPECT imaging, therefore, the regional decrease in uptake of I-123 iomazenil indicates the location of epileptogenic foci. Similar findings on I-123 iomazenil SPECT, however, are also observed in brain regions with thin cortical ribbons, gray matter atrophy, or other pathologic brain changes. This limitation is caused by the PVE, which arises from the limited spatial resolution of the scanner. In small structures, the observed radioactivity concentration differs from the true concentration because of blurring of the counts out of the structure ("spill-out") and blurring of the counts into the structure from the surrounding radioactivity ("spill-in").[4] We have created I-123 iomazenil SPECT images corrected for the whole-brain gray matter volume on the basis of MR imaging measurements in a small number of patients with intractable partial epilepsy and have suggested that the detectability of cortical epileptogenic foci improved in this previous study.[5] In the present study, we carried out the investigation with a much larger number of patients to establish the improvement of foci detectability with I-123 iomazenil SPECT by MR imaging–based PVE correction.

Received January 10, 2012; accepted after revision February 26.

From the Department of Nuclear Medicine and Tracer Kinetics (H.K., E.S., K.I., J.H.), Osaka University Graduate School of Medicine, Osaka, Japan; National Epilepsy Center (K.M., K.B.), Shizuoka Institute of Epilepsy and Neurological Disorders, Shizuoka, Japan; and World Premier International Immunology Frontier Research Center (M.I.), Osaka University, Osaka, Japan.

Contributions of each author: Hiroki Kato: conception, design, analyzing and interpreting data, and drafting the manuscript; Kazumi Matsuda: conception and design and revising the manuscript; Koich Baba: acquiring data and enhancing intellectual content; Eku Shimosegawa: enhancing intellectual content; Kayako Isohashi: enhancing intellectual content; Masao Imaizumi: enhancing intellectual content; Jun Hatazawa: conception and design and critically contributing to the manuscript.

This study was partially supported by the Ministry of Education, Culture, Sports, Science, and Technology Grant-in-Aid for Scientific Research (C) (No. 23592089) in Japan.

Please address correspondence to Hiroki Kato, MD, PhD, Department of Nuclear Medicine and Tracer Kinetics, Osaka University Graduate School of Medicine, 2–2, Yamadaoka, Suita, Osaka, 565-0871, Japan; e-mail:kato-h@umin.ac.jp

http://dx.doi.org/10.3174/ajnr.A3121

Materials and Methods

Patients

Seventy-five consecutive patients (male/female, 37/38; age, 28 ± 12 years; duration of illness, 17 ± 11 years) at the Shizuoka Institute of Epilepsy and Neurologic Disorder, which is the largest facility for the treatment of and research on intractable epilepsy in Japan, were ret-

rospectively enrolled in this study. All the subjects had intractable epilepsy and met the following criteria: 1) no significant morphologic brain lesion that could disturb automatic segmentation or spatial normalization on 3D MR imaging; 2) surgical removal and histopathologic examination of suspected epileptogenic foci performed; 3) I-123 iomazenil brain SPECT and 3D T1-weighted MR imaging studies performed before the operation; and 4) marked improvement of symptoms after surgery, with the seizure outcome at the 2-year follow-up being as good as or better than Engel class II.[6] The rationale for selecting only patients with good surgical outcomes is explained in "Visual Assessment" in this section.

The patient clinical information is summarized in Table 1. All patients had complex partial seizures with or without generalization and were being treated with anticonvulsants. All patients underwent extracranial scalp video-EEG (interictal and ictal recording) to identify the location and extent of the epileptogenic foci. All the specimens resected during the operations were histopathologically investigated.

The study was approved by the Ethical Committee of Shizuoka Institute of Epilepsy and Neurologic Disorder for clinical research.

SPECT

In each subject, 167 MBq of I-123 iomazenil was intravenously administered. Three hours after the injection, SPECT image acquisition was performed while the subject rested in a quiet room in a supine position on the scanning bed with his or her eyes closed. The SPECT scanning was performed by using a dual-head multigeometry nuclear medicine camera (Millennium VG; GE Healthcare Japan, Tokyo, Japan) with a parallel type collimator (low energy general purpose). The SPECT acquisition protocol was 50 seconds per step, with 36 collections over 360°, and the data were recorded in a 128 × 128 matrix. The raw SPECT data were transferred to a nuclear medicine computer and then processed by Xeleris software (GE Healthcare Japan). The projection data were prefiltered by using a Butterworth filter (cutoff frequency, 0.35 cycles/pixel; order 10) and reconstructed into transaxial sections of 3.16-mm-thick images in planes parallel to the orbitomeatal line. Attenuation correction was performed by using the Chang method[6] with an optimized effective attenuation coefficient of 0.11 cm^{-1}.

PVE Correction

PVE correction was performed by using a method similar to that described in our previous pilot study.[5] In this section and in Fig 1, the method for PVE correction and anatomical normalization are briefly described. 3D T1-weighted MR imaging was performed by a Genesis Signa 1.5T scanner (GE Healthcare Japan) by using a fast-spoiled gradient-recalled sequence (TE/TR, 5.15/11.9 ms; flip angle, 20°; acquisition matrix, 256 × 256; section thickness, 2.0 mm). The 3D T1-weighted MR imaging was first segmented into gray matter and other compartments and was then anatomically normalized by using the unified model[8] of Statistical Parametric Mapping 5 (Wellcome Department of Imaging Neuroscience: http://www.fil.ion.ucl.ac.uk/spm/) according to the optimized voxel-based morphometry protocol.[10] These procedures generated both spatial-normalization matrices and inverse spatial-normalization matrices.

The normalized gray matter maps yielded in the above procedures were transformed into native space by using inverse spatial-normalization matrices. The native space gray matter maps thus produced were subsequently binarized (given a value of 0 for the absence of gray matter or 1 for the presence of gray matter),[11] and are referred to as "binarized gray matter maps." The binarized gray matter maps were convoluted with a 3D Gaussian function with a full width at half maximum of 16 × 16 × 16 mm, which was assumed to be the same as the point-spread function of the reconstructed SPECT image, as described in previous studies.[12,13] The resulting image is subsequently referred to as the "smoothed gray matter map." The SPECT images

Table 1: Demographics of the patients

Demographic	No.
Total	75
Focus laterality	
Right	35
Left	40
Focus location	
Temporal	57
Frontal	13
Parietal	1
Occipital	2
Temporo-occipital	1
Parieto-occipital	1
Histologic diagnosis	
MTS	34
MCD	
Cortical dysplasia	8
Tuberous sclerosis	2
Heterotopia	1
Tumor	
Glioma	8
Ganglioglioma	3
Amygdalar hamartoma	3
Angioma	3
DNT	3
Nonspecific	
No remarkable abnormality	8
Atrophy	2
Prognosis (Engel classification)[a]	
Ia	44
Ib	9
Ic-d	0
IIa	0
IIb	22
IIc-d	0
III	0
IV	0
Medication[b]	
CBZ	52
PHT	34
PB	18
VPA	11
CLB	14
DZP	1
CZP	4
Application of invasive EEG[c]	
No	52
Yes	23

Note:—DNT indicates dysembryoplastic neuroepithelial tumor; CBZ, carbamazepine; PHT, phenytoin; PB, phenobarbital; VPA, sodium valproate; CLB, clobazam; DZP, diazepam; CZP, clonazepam.
[a] Class I: Free of disabling seizures. a, Completely seizure-free since surgery. b, Nondisabling simple partial seizures only since surgery. c, Some disabling seizures after surgery, but free of disabling seizures for at least 2 years. d, Generalized convulsions with antiepileptic drug discontinuation only. Class II: Rare disabling seizures. ("almost seizure-free") a, Initially free of disabling seizures but has rare seizures now. b, Rare disabling seizures since surgery. c, More than rare disabling seizures since surgery, but rare seizures for the last 2 years. d, Nocturnal seizures only. Class III: Worthwhile improvement. a, Worthwhile seizure reduction. b, Prolonged seizure-free intervals amounting to greater than half the follow-up period, but not <2 years. Class IV: No worthwhile improvement. a, Significant seizure reduction. b, No appreciable change. c, Seizures worse.
[b] Use of anticonvulsants at the time of I-123 iomazenil SPECT examination.
[c] Group of patients who underwent 2-step surgery: intracranial EEG electrode implantation and foci resection. This group comprised 5 cases of MTS, 6 cases of MCD, 7 tumors, and 5 healthy patients.

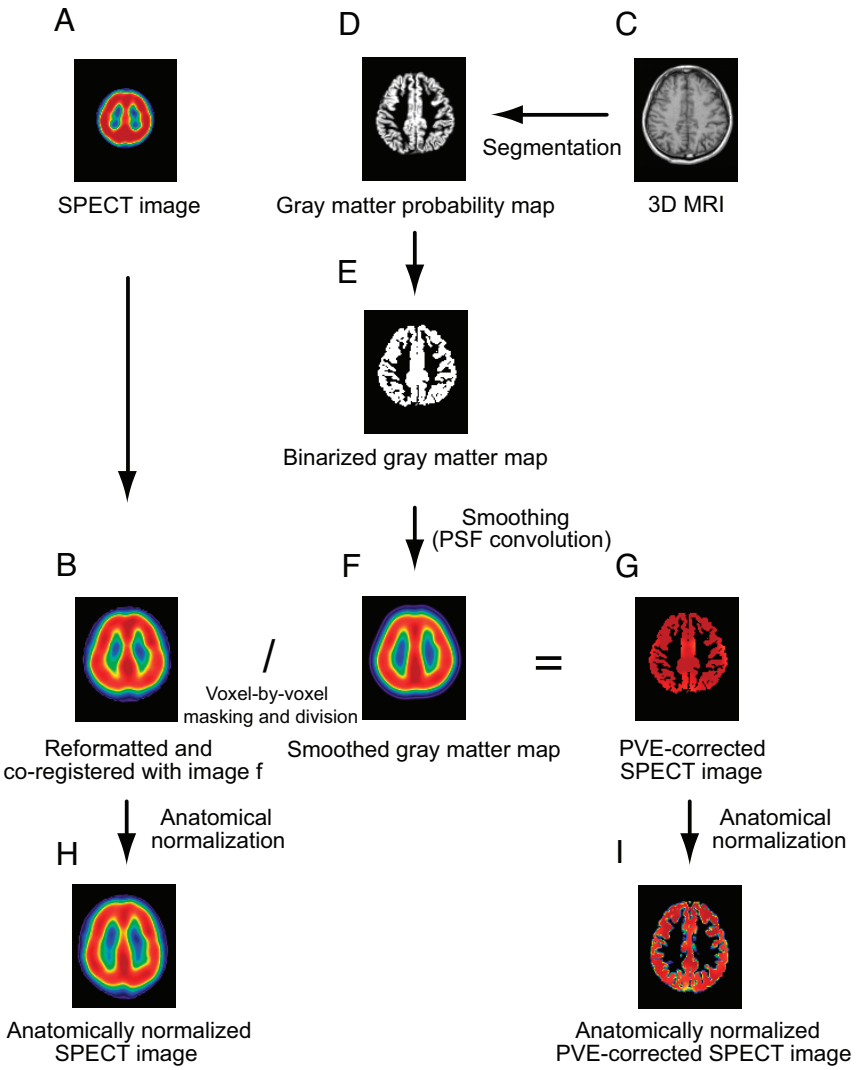

Fig 1. *A,* I-123 iomazenil SPECT image. *B,* Automatic coregistration of the I-123 SPECT image with the MR image. The maps are simultaneously reformatted to a matrix that is the same size as the referenced smoothed gray matter map. *C,* 3D MR image obtained before surgery. *D,* The MR image is segmented into a gray matter map. *E,* The gray matter probability map is subsequently binarized. *F,* Binary map for gray matter convoluted with the point-spread function (smoothed gray matter map). *G,* Smoothed gray matter map masked by the image *E.* The coregistered I-123 SPECT image is divided by using the masked smoothed gray matter map on a voxel-by-voxel basis. *H,* Image *B* anatomically normalized by the spatial normalization matrices generated in the segmentation process. *I,* Image *G* anatomically normalized in the same manner as image *H.*

were coregistered to the smoothed gray matter maps by using the Linear Image Registration Tool of Functional MR Imaging of the Brain (www.fmrib.ox.ac.uk/fsl).[14] The coregistered SPECT image was masked with the binarized gray matter map. The masked SPECT image was then divided by using the smoothed gray matter map on a voxel-by-voxel basis to make the PVE-corrected SPECT image (Fig 1). Masking with a binarized gray matter map was performed to prevent irrelevant results caused by division by low gray matter concentration in the regions corresponding to white matter. The SPECT images before and after PVE correction were anatomically normalized by the corresponding spatial-normalization matrices generated in the segmentation and normalization procedure previously mentioned.

Visual Assessment

Six experienced nuclear medicine physicians performed visual assessments of the SPECT images. The physicians were unaware of the patient clinical information to avoid biases caused by differences in the amount of information available for each patient. The physicians visually evaluated the transaxial and/or coronal sections of anatomically normalized I-123 iomazenil SPECT images with and without the PVE correction, presented in a random order, and noted the areas of epileptogenic foci, where the tracer uptake was reduced compared with the corresponding contralateral regions. Decisions regarding the foci were made by joint agreement during a conference of the 6 physicians. Apart from the conference, a brief interobserver reliability test for separate visual assessments by 2 physicians was also performed in the same manner as described.

To identify the resected lesion in the normalized space, an MR image acquired in the stable phase after surgery was first coregistered to the 3D MR image acquired before surgery and was anatomically normalized by the corresponding spatial-normalization matrices generated in the procedure mentioned in the previous section. In the present study, the sensitivity and specificity of the foci detection were determined on a patient-by-patient basis. In the present study, as described under "Patients," only those patients who showed markedly good surgical outcomes were enrolled (Table 1); we can assume, therefore, that the resected lesions corresponded to the true epileptogenic foci and that the unresected regions corresponded to the intact

Table 2: Evaluation criteria for visual assessment of SPECT

	Resected Brain Region	Unresected Brain Region
SPECT positive[a]	True-positive	False-positive
SPECT negative[b]	False-negative	True-negative

[a] SPECT count decrease detected in the brain region by visual assessment.
[b] No count decrease in the brain region.

brain. Then, a "true-positive " case was defined as a case with visually detected foci in a resected brain region, a "true-negative " case was defined as a case without visually detected foci in an unresected brain region, a "false-positive " case was defined as a case with visually detected foci in an unresected brain region, and a "false-negative case " was defined as a case without visually detected foci in a resected brain region (Table 2). The sensitivity, specificity, and accuracy of uncorrected or PVE-corrected SPECT images were calculated as follows:

sensitivity = number of true-positive cases / total number of patients

specificity = number of true-negative cases / total number of patients

accuracy = number of cases of true-positive and true-negative at the same time / total number of patients.

Comparison of sensitivity, specificity, and/or accuracy between the uncorrected and the PVE-corrected images was performed by using the McNemar test.

Quantitative Assessment

Quantitative assessment based on asymmetry of the SPECT count in the foci was performed to evaluate the effect of PVE correction. First, the uniform size of the spheric VOI was established and located in the center of the resected lesion in reference to an MR image acquired after the surgery (Fig 2). For each of these VOIs, the corresponding contralateral congruent VOI was located at the symmetric position based on the Montreal Neurological Institute coordinates. Voxels with zero or negative values were eliminated from the VOI to avoid the pickup of irrelevant voxels. The VOI counts of the uncorrected or the PVE-corrected SPECT images were measured to evaluate the change in asymmetry of the SPECT count in the visually detected epileptogenic foci. The AI for the I-123 iomazenil count of the ipsilateral VOI A C_A and that of the contralateral VOI B C_B was calculated as follows:

$$AI_{(\%)} = |C_A - C_B| \times 200/ (C_A + C_B).$$

In each case, the CV of the whole brain SPECT counts before and after PVE correction were measured to correct the above-mentioned AI values for the dispersion of voxel values in the whole-brain images. Apart from the foci VOI described above, a whole-brain VOI including only the voxels with positive value in both the uncorrected and the PVE-corrected images was made for each case. As for the uncorrected and PVE-corrected images, CV(%) of the voxel values included in the whole-brain VOI and subsequently AI(%) / CV(%) were calculated. Comparison of AI and/or AI/CV between the uncorrected and the PVE-corrected images was performed by using the Wilcoxon signed rank test.

Results

Visual Assessment

The inter-rater concordance of visual assessment was good; the κ value was 0.6 for uncorrected SPECT and 0.85 for PVE-corrected SPECT. As a result of visual assessment for change in foci detectability by SPECT PVE correction, sensitivity, specificity, and accuracy were significantly improved for all patients after PVE correction (Table 3 and Fig 3). For the cases of MTS or tumor, sensitivity and accuracy were significantly improved after PVE correction. Sensitivity and accuracy were significantly improved for the foci in the mesial temporal area after PVE correction. For the foci in the neocortical area, sensitivity, specificity, and accuracy were significantly improved. Sensitivity and accuracy were significantly improved for the patients in the MTS group or for those with tumor after PVE correction. Sensitivity and accuracy were significantly improved by PVE correction for the 23 patients who underwent invasive EEG using depth electrodes and/or subdural electrodes before resection surgery because of inconsistent results of presurgical examinations.

Quantitative Assessment

As a result of quantitative assessment, AIs in foci were significantly increased by SPECT PVE correction in cases with MCD and tumor. AI/CV, moreover, was increased by SPECT PVE correction in the cases with MTS, MCD, and tumor. In cases without abnormal histologic findings except for slight atrophy, on the other hand, no significant changes in AI or AI/CV by PVE correction were observed (Table 4).

Discussion

We report that the MR imaging–based PVE correction method for I-123 iomazenil SPECT improved detectability of epileptogenic foci in the present study on the basis of a much larger number of patients than that in our previous pilot study.[7] In this study, foci detectability of uncorrected or PVE-corrected SPECT images was evaluated in each subgroup on the basis of the location or histologic diagnosis of the foci. As a result of visual assessment, PVE correction significantly improved foci detectability of I-123 iomazenil SPECT both in the neocortical and mesial temporal areas. As for specificity of foci detection by SPECT, significant improvement was observed in the neocortical area after PVE correction. This is because PVE tends to be more prominent in the neocortical area under the influence of more complicated and sparser sulcal structures than in the mesial temporal area, and the influence can be effectively removed by PVE correction. In the cases of MTS and of tumor, accuracy of foci detectability was significantly improved by PVE correction. In the cases of MCD, improvement of detectability was remarkable, though it failed to reach significance. This result may be accounted for by the relatively small sample size of the group. For the patient group with no abnormal histologic findings but focal atrophy, on the other hand, foci detectability was not markedly changed by PVE correction. The effect of PVE correction for SPECT on foci detection seems to relate to histologic abnormality of the foci.

One-step surgery for foci resection was performed if the epileptogenic foci were successfully detected on the basis of consistent results of presurgical examinations; otherwise, invasive EEG using depth electrodes and/or subdural electrodes was performed before the resection surgery because of inconsistent results of presurgical examinations. Sensitivity and accuracy of foci detection by uncorrected SPECT were remarkably lower in the latter cases than in the former ones; foci

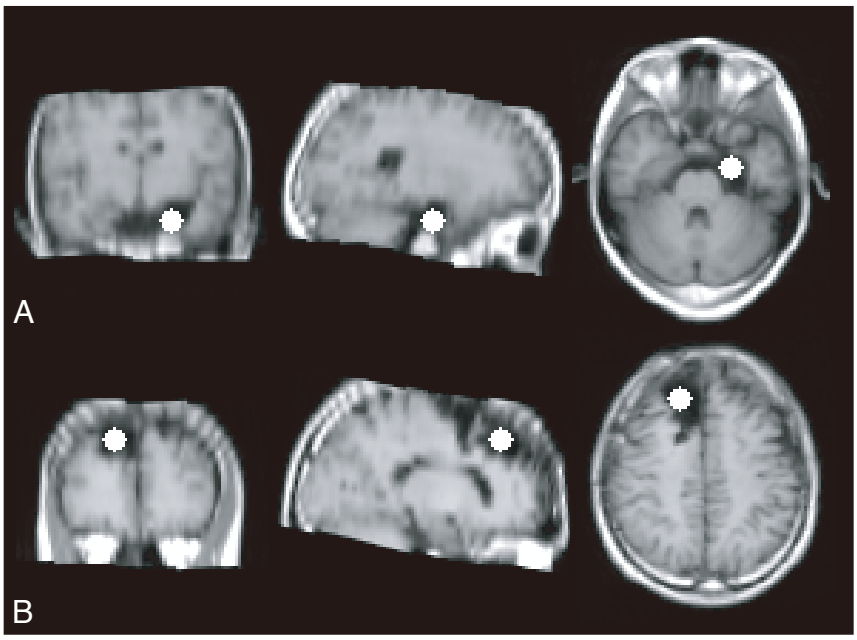

Fig 2. Samples of the VOI set in the left mesial temporal lesion (*A*) and the right frontal lesion (*B*). The uniform size of spheric VOI was established. The size of the VOI (16 mm in diameter) was determined so as to be included in any resected lesion and located in the center of the resected lesion in reference to an MR image acquired after the surgery.

Table 3: Results of the visual assessment of foci detectability

		Sensitivity (%)			Specificity (%)			Accuracy (%)		
	No.	Pre-PVC	Post-PVC	*P*	Pre-PVC	Post-PVC	*P*	Pre-PVC	Post-PVC	*P*
Total	75	49	85	<.001	69	85	.003	43	84	<.001
Histologic diagnosis										
MTS	34	70	93	.004	90	93	NS	67	93	.001
MCD	11	50	90	NS	60	80	NS	30	80	.06
Tumor	20	28	83	<.001	56	83	.06	28	83	<.001
Nonspecific	10	40	60	NS	40	60	NS	30	60	NS
Foci location										
Mesial temporal	41	56	90	<.001	78	90	NS	51	90	<.001
Neocortex	34	41	79	<.001	59	79	.03	32	76	<.001
Invasive EEG										
No[a]	52	56	90	<.001	73	88	.01	48	88	<.001
Yes[b]	23	35	74	.004	61	78	NS	30	74	.002

Note:—PVC indicates partial volume correction; NS, not significant.
[a] Application of the 1-step resection surgery without invasive EEG.
[b] Application of both invasive EEG and resection surgery.

detectability was, on the other hand, significantly improved by PVE correction even in the latter cases. This finding suggests that some of the latter cases could be treated by 1-step surgery without invasive EEG, if the PVE-corrected SPECT was used to detect foci.

The AI in the foci was significantly increased by PVE correction for the patient group with MCD and tumor. Increase in AI after PVE correction implies the following 2 factors: One is decrease in the SPECT count in the foci compared with the corresponding contralateral area, and the other is an increase in the volume of the gray matter and/or a decrease in the volume of the adjacent white matter in the lesion areas compared with that in the corresponding contralateral normal areas.[7] In cases of MCD, decrease in inhibitory synaptic connectivity[15] or altered transcription of genes encoding GABAergic receptors[16] has been reported. In a previous study,[17] on the other hand, increase in the regional gray matter concentration in MCD was detected in patients with focal cortical dysplasia by voxel-based morphometry.[18] The case of subcortical heterotopia indicated in Fig 3*C* is thought to be a representative example. In cases of tumor, underexpressed GABA-receptor signaling in gangliogliomas,[19] (GABA)A-central low benzodiazepine receptor binding in dysembryoplastic neuroepithelial tumors,[20] or a significant decrease in GABAergic-immunoreactive neurons in low-grade gliomas[21] has been reported.

As a result of tumor cell proliferation, regional gray matter concentration in the foci is naturally increased in cases of tumor. Thus, in cases of MCD or tumor, our results of analysis for AI change by PVE correction can be accounted for by these findings about central benzodiazepine receptor binding or the results of voxel-based volumetric analysis. In cases of hippocampal sclerosis, attenuation of the central benzodiazepine receptor in the mesial temporal region has been reported to be decreased.[1] Previous voxel-based morphometry studies have demonstrated not only a change of regional gray matter concentration but also a change of regional white matter concen-

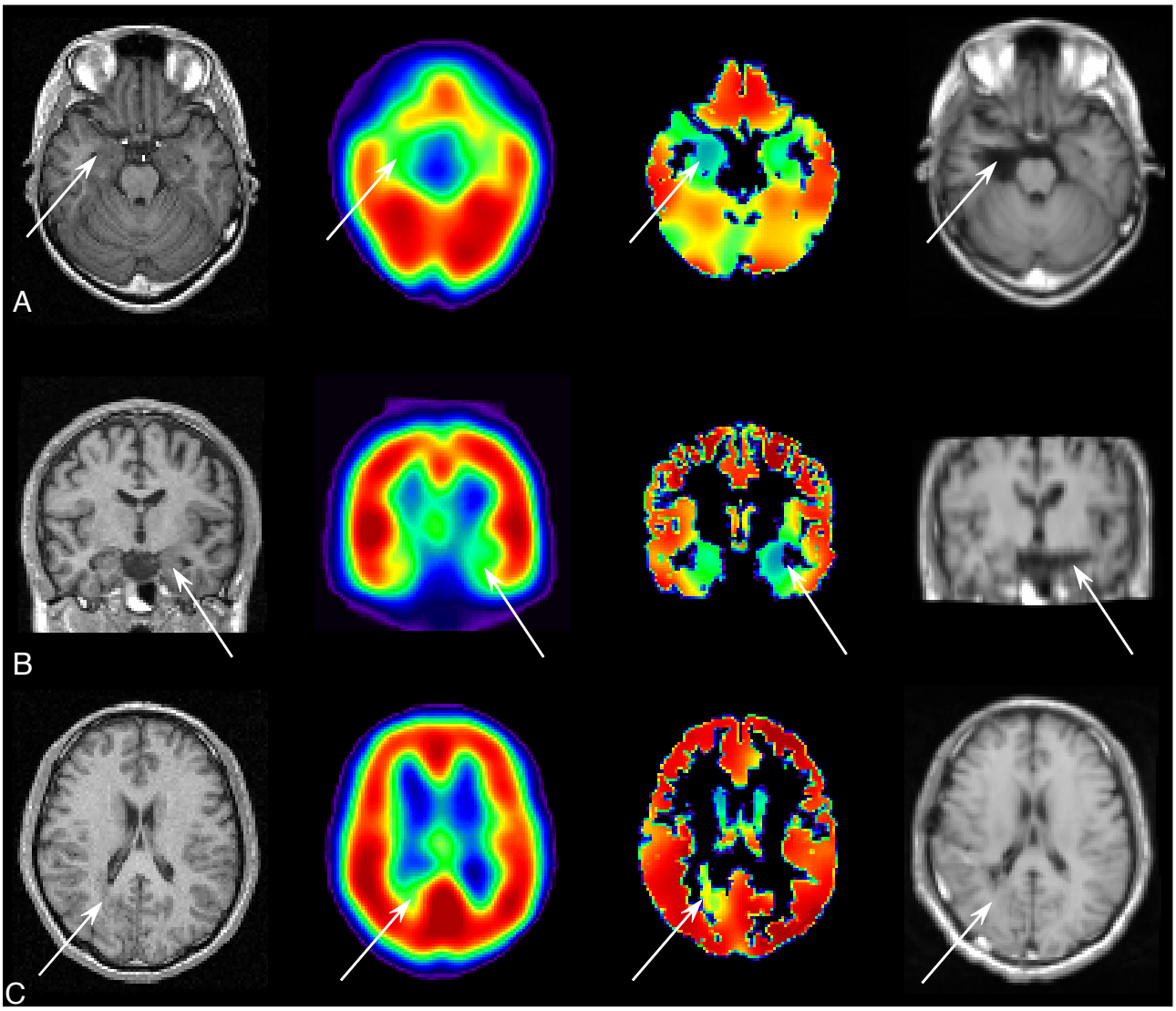

Fig 3. MR imaging acquired before surgery (far left column), uncorrected SPECT (the second column from the left), PVE-corrected SPECT (the third column from the left), and MR imaging acquired after surgery (far right column). Arrows indicate the location of resected lesions. *A*, A case of glioma without any remarkable findings in the uncorrected SPECT, showing a count decrease detected in the PVE-corrected SPECT in the right mesial temporal region. Right mediobasal temporal corticectomy was performed and the postoperative outcome after a 2-year follow-up period was Engel class Ia. *B*, A case of mesial temporal sclerosis without any remarkable findings in the uncorrected SPECT, showing a count decrease in the PVE-corrected SPECT in the left mesial temporal region. Left selective amygdalohippocampectomy was performed and the postoperative outcome after 2-year follow-up was Engel class Ia. *C*, A case of heterotopias showing a slight increase in the uncorrected SPECT and a count decrease in the PVE-corrected SPECT in the right temporo-occipital subcortical region. Lesionectomy in the temporo-occipital subcortical area was performed, and the postoperative outcome after 2-year follow-up was Engel class Ia.

Table 4: Results of the quantitative assessment based on asymmetry of SPECT counts

		Mean AI (%) (SD)			Mean AI (%)/CV (%) (SD)		
Histologic Diagnosis	No.	Pre-PVC	Post-PVC	*P*	Pre-PVC	Post-PVC	*P*
MTS	34	23 (16)	22 (16)	NS	0.76 (0.52)	1.1 (0.80)	<.001
MCD	11	18 (17)	25 (17)	.01	0.55 (0.49)	1.3 (0.82)	<.001
Tumor	20	14 (15)	17 (16)	<.001	0.44 (0.43)	0.89 (0.81)	<.001
Nonspecific	10	16 (22)	14 (16)	NS	0.62 (0.98)	0.72 (0.83)	NS

Note:—NS indicates not significant.

tration in the mesial temporal area ipsilateral to the foci. A study showed significant increase in gray matter concentration in the ipsilateral temporal area,[18] whereas another study demonstrated decrease in gray matter concentration in a very small area in the ipsilateral mesial temporal lobe by using the optimal voxel-based morphometry method.[22] White matter reduction, on the other hand, was reported in the mesial temporal area ipsilateral to the seizure foci.[23] In the present study, no significant AI change by PVE correction was observed, which seems to reflect the conflicting results of previous studies by volumetric analysis for gray matter concentration in the foci. AI/CV, on the other hand, was significantly increased for all the patient groups with abnormal histologic findings. This finding implies that PVE correction enables the pathologic

SPECT-count reduction to be recognized by suppressing apparent fluctuations in the count caused by the distribution of gray matter. This result of quantitative analysis accounts for the improvement of foci detectability by visual assessment. In the cases with no abnormal histologic findings, however, no significant change of AI or AI/CV was found, which is consistent with the results of visual assessment.

The present study has some limitations. First, in this study, patients with significant structural abnormalities detected on MR imaging were eliminated to avoid disturbance in automatic segmentation, coregistration, and spatial normalization. Although MR imaging is one of the most reliable modalities for the detection of epileptogenic foci, SPECT may play a more important role in patients with minor structural abnormalities than in those with major structural abnormalities of the brain.

Second, some patients were taking anticonvulsants at the time of their I-123 iomazenil SPECT examination (Table 1), even though such drugs may influence iomazenil binding to a certain extent. As discussed in our previous study,[7] however, the extent of this influence is rather small.

Third, the method of PVE correction used in this study diminishes anatomic information woven into the original SPECT images, instead of canceling out PVE-related modification of SPECT counts. To compensate for this problem, we normalized all the images to the common Montreal Neurological Institute template. For clinical use, however, it may be necessary to refer to the coregistered MR imaging.

Fourth, because all subjects were patients with epileptogenic lesions, it would seem difficult to assess the absolute ability, per se, of I-123 iomazenil SPECT to exclude normal asymmetry of central benzodiazepine receptor binding. We have also performed an asymmetry analysis of normal central benzodiazepine receptor binding, and the report is currently under preparation.

Fifth, the present study is a retrospective one, which is inevitably affected by the bias of patient selection for analysis. We have already started a prospective study in major institutions in Japan that are treating large numbers of patients with intractable epilepsy.

Sixth, the MR imaging–based PVE correction scheme applied here is known to be sensitive to the effects of misregistration and mis-segmentation,[24] though, at poor spatial resolution like SPECT, the impact of these effects on PVE correction is relatively small.[25] To date, several methods to correct for PVEs have been proposed.[24,26,27] Among these, the voxel-based and MR imaging–based PVE correction scheme is the most feasible for operative clinical implementation because it is simple, less time consuming, and suitable for visual detection of the foci in the whole range of cerebral cortices; moreover, MR imaging examinations are routinely executed for presurgical diagnosis of epileptogenic foci in most cases of intractable epilepsy.

Conclusions

In the present study, we established the effectiveness of MR imaging–based PVE correction in I-123 iomazenil brain SPECT in improving the detection of cortical epileptogenic foci with abnormal histologic findings by investigation of a large number of patients with intractable partial epilepsy and suggest the possibility that a more invasive examination could be avoided in some cases by the use of this technique.

Acknowledgments

We thank the staff of the Shizuoka Institute of Epilepsy and Neurologic Disorders for their technical support in performing the studies.

References

1. Sata Y, Matsuda K, Mihara T, et al. **Quantitative analysis of benzodiazepine receptor in temporal lobe epilepsy: [(125)I]iomazenil autoradiographic study of surgically resected specimens.** *Epilepsia* 2002;43:1039–48
2. Beer HF, Blauenstein PA, Hasler PH, et al. **In vitro and in vivo evaluation of iodine-123-Ro 16–0154: a new imaging agent for SPECT investigations of benzodiazepine receptors.** *J Nucl Med* 1990;31:1007–14
3. Morimoto K, Watanabe T, Ninomiya T, et al. **Quantitative evaluation of central-type benzodiazepine receptors with [(125)I]Iomazenil in experimental epileptogenesis: II. The rat cortical dysplasia model.** *Epilepsy Res* 2004;61:113–18
4. Hoffman EJ, Huang SC, Phelps ME. **Quantitation in positron emission computed tomography. 1. Effect of object size.** *J Comput Assist Tomogr* 1979;3:299–308
5. Kato H, Shimosegawa E, Oku N, et al. **MRI-based correction for partial-volume effect improves detectability of intractable epileptogenic foci on 123I-iomazenil brain SPECT images.** *J Nucl Med* 2008;49:383–89
6. Engel J Jr, Van Ness P, Rasmussen TB, et al. **Outcome with respect to epileptic seizures.** In: Engel J Jr, ed. *Surgical Treatment of the Epilepsies.* New York: Raven Press; 1993:609–21
7. Chang LT. **A method for attenuation correction in radionuclide computed tomography.** *IEEE Trans Nucl Sci* 1978;25:638–43
8. Ashburner J, Friston KJ. **Unified segmentation.** *Neuroimage* 2005;26:839–51
9. Good CD, Johnsrude IS, Ashburner J, et al. **A voxel-based morphometric study of ageing in 465 normal adult human brains.** *Neuroimage* 2001;14:21–36
10. Ashburner J, Friston KJ. **Voxel-based morphometry: the methods.** *Neuroimage* 2000;11:805–21
11. Bencherif B, Stumpf MJ, Links JM, et al. **Application of MRI-based partial-volume correction to the analysis of PET images of mu-opioid receptors using statistical parametric mapping.** *J Nucl Med* 2004;45:402–08
12. Matsuda H, Ohnishi T, Asada T, et al. **Correction for partial-volume effects on brain perfusion SPECT in healthy men.** *J Nucl Med* 2003;44:1243–52
13. Ibanez V, Pietrini P, Alexander GE, et al. **Regional glucose metabolic abnormalities are not the result of atrophy in Alzheimer's disease.** *Neurology* 1998;50:1585–93
14. Jenkinson M, Smith S. **A global optimisation method for robust affine registration of brain images.** *Med Image Anal* 2001;5:143–56
15. Zhou FW, Roper SN. **Densities of glutamatergic and GABAergic presynaptic terminals are altered in experimental cortical dysplasia.** *Epilepsia* 2010;51:1468–76
16. White R, Hua Y, Scheithauer B, et al. **Selective alterations in glutamate and GABA receptor subunit mRNA expression in dysplastic neurons and giant cells of cortical tubers.** *Ann Neurol* 2001;49:67–78
17. Bonilha L, Montenegro MA, Rorden C, et al. **Voxel-based morphometry reveals excess gray matter concentration in patients with focal cortical dysplasia.** *Epilepsia* 2006;47:908–15
18. Woermann FG, Free SL, Koepp MJ, et al. **Voxel-by-voxel comparison of automatically segmented cerebral gray matter: a rater-independent comparison of structural MRI in patients with epilepsy.** *Neuroimage* 1999;10:373–84
19. Aronica E, Boer K, Becker A, et al. **Gene expression profile analysis of epilepsy-associated gangliogliomas.** *Neuroscience* 2008;151:272–92
20. Richardson MP, Hammers A, Brooks DJ, et al. **Benzodiazepine-GABA(A) receptor binding is very low in dysembryoplastic neuroepithelial tumor: a PET study.** *Epilepsia* 2001;42:1327–34
21. Haglund MM, Berger MS, Kunkel DD, et al. **Changes in gamma-aminobutyric acid and somatostatin in epileptic cortex associated with low-grade gliomas.** *J Neurosurg* 1992;77:209–16
22. Keller SS, Wilke M, Wieshmann UC, et al. **Comparison of standard and optimized voxel-based morphometry for analysis of brain changes associated with temporal lobe epilepsy.** *Neuroimage* 2004;23:860–68
23. Bernasconi N, Duchesne S, Janke A, et al. **Whole-brain voxel-based statistical analysis of gray matter and white matter in temporal lobe epilepsy.** *Neuroimage* 2004;23:717–23
24. Quarantelli M, Berkouk K, Prinster A, et al. **Integrated software for the analysis of brain PET/SPECT studies with partial-volume-effect correction.** *J Nucl Med* 2004;45:192–201
25. Meltzer CC, Kinahan PE, Greer PJ, et al. **Comparative evaluation of MR-based partial-volume correction schemes for PET.** *J Nucl Med* 1999;40:2053–65
26. Rousset OG, Ma Y, Evans AC. **Correction for partial volume effects in PET: principle and validation.** *J Nucl Med* 1998;39:904–11
27. Soret M, Bacharach SL, Buvat I. **Partial-volume effect in PET tumor imaging.** *J Nucl Med* 2007;48:932–45